ACS APPLIED MATERIALS & INTERFACES

Research Article

www.acsami.org

High-Performance Supercapacitors Based on Hollow Polyaniline Nanofibers by Electrospinning

Yue-E Miao, Wei Fan, Dan Chen, and Tianxi Liu*

State Key Laboratory of Molecular Engineering of Polymers, Department of Macromolecular Science, Fudan University, Shanghai 200433, PR China

ABSTRACT: Hollow polyaniline (PANI) nanofibers with controllable wall thickness are fabricated by in situ polymerization of aniline using the electrospun poly(amic acid) fiber membrane as a template. A maximum specific capacitance of 601 F g^{-1} has been achieved at 1 A g^{-1}, suggesting the potential application of hollow PANI nanofibers for supercapacitors. The superior electrochemical performance of the hollow nanofibers is attributed to their hollow structure, thin wall thickness, and orderly pore passages, which can drastically facilitate the ion diffusion and improve the utilization of the electroactive PANI during the charge−discharge processes. Furthermore, the high flexibility of the self-standing fiber membrane template provides possibilities for the facile construction and fabrication of conducting polymers with hollow nanostructures, which may find potential applications in various high-performance electrochemical devices.

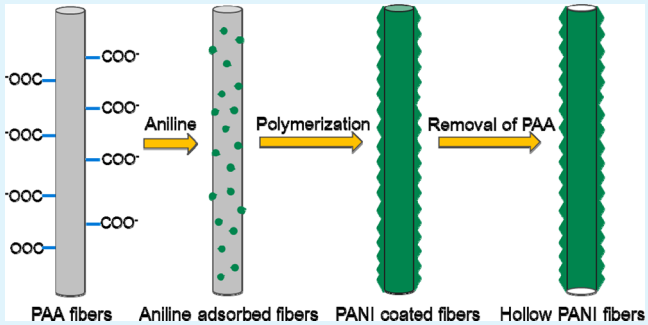

KEYWORDS: *electrospinning, template, hollow nanofibers, supercapacitors*

1. INTRODUCTION

In recent years, electrochemical supercapacitors have aroused broad interests due to the strong demand for lightweight and flexible portable energy management in the rapidly growing world ecology and economy.[1,2] As a new type of promising modern energy storage system, the supercapacitors are quite different from the traditional capacitors, which combine the advantages of both conventional dielectric capacitors and rechargeable batteries to obtain high power density, long durability, and good operational safety. Therefore, the performance of these devices heavily relies on the physical and chemical properties of their electrode materials.[3,4] It is well-known that polyaniline (PANI) is one of the most useful conducting polymers. Due to its ease of synthesis, good environmental stability, high conductivity and theoretical specific capacitance, PANI has been widely used in supercapacitor electrode materials.[5−7] Nevertheless, the electrochemical performance of the conducting polymer is unsatisfactory under high mass loadings. With the mass loading increases, PANI becomes densely packed with the decreased accessible surface area, thus resulting in limited participation of the conducting polymer in the charge storage process and comparatively low specific capacitance.[5] Therefore, porous or hollow-structured materials with enhanced surface-to-volume ratio and reduced distance for mass and charge transport are considered as one new type of promising material for applications in energy-related systems.[8−10] Thus, the development of hierarchically structured PANI nanomaterials with high specific surface area, high electrical conductivity, and a fast ion diffusion process is of great importance to achieve predominant electrochemical performance.

Thus far, various hierarchically structured PANI nanomaterials, such as nanotube arrays, hollow microspheres, and needle-like nanowires, have been successfully obtained with excellent electrochemical performance.[11−14] Wang et al. developed an electrochemical deposition route for the synthesis of polyaniline nanotube arrays using the electrodeposited ZnO nanorods as template. The as-prepared polyaniline nanotube arrays exhibit a high capacitance value of 675 F g^{-1} and retention ratio of 70% after 400 cycles at a scan rate of 50 mV s^{-1}.[15] Lei et al. obtained polyaniline coated hollow carbon sphere (HCS) composites through the chemical oxidative polymerization of aniline in the presence of HCS, which achieved a capacitance value of 525 F g^{-1}.[16] Cao et al. also studied the electrochemical growth of polyaniline on anodic aluminum oxide membranes to obtain open-structured polyaniline nanowires for high-performance supercapacitors.[17] Nevertheless, the development of facile and effective methods to obtain PANI with hollow nanostructures is still a great challenge.

Electrospinning is a promising and straightforward technique that produces continuous fibers with diameters in the range of nanometers to a few micrometers. Electrospun fibers thus obtained possess high surface area to volume ratio, high porosity, and other outstanding properties, making them an

Received: March 6, 2013
Accepted: April 15, 2013
Published: April 15, 2013

   dx.doi.org/10.1021/am4008352 | ACS Appl. Mater. Interfaces 2013, 5, 4423−4428

excellent matrix or template to fabricate various hierarchical nanostructures for sensors, catalysts, remediation, and energy storage applications.[18−23] Zhi et al. reported the highly conductive carbon nanofiber/MnO_2 coaxial cables in which individual electrospun carbon nanofibers are coated with an ultrathin MnO_2 layer. The as-obtained composites with hierarchical structures exhibit good cycling stability, high energy density (80.2 Wh kg^{-1}), and high power density (57.7 kW kg^{-1}).[24] Mu et al. obtained highly dispersed Fe_3O_4 nanosheets on one-dimensional carbon nanofibers through the combination of electrospinning and a solvent-thermal process, which shows great potentials for high-performance supercapacitors.[25] Poly(amic acid) (PAA), the precursor of polyimide, is soluble in organic solvents and can be easily prepared into uniform fibers with controllable diameters.[26] The −COOH groups of PAA endow the electrospun fiber membrane with good hydrophilicity, which makes it an excellent template to capture electropositive molecules through electrostatic attraction in aqueous solutions.[27,28] Therefore, in this study, PAA/PANI core/shell nanofibers with controllable diameters are fabricated by in situ polymerization of aniline using the electrospun PAA fiber membrane as a template, which is followed by removal of the PAA core to form hollow nanofibers of PANI. Electrochemical experiments show that a maximum specific capacitance of 601 F g^{-1} is achieved at 1 A g^{-1}, suggesting the potential application of hollow PANI nanofibers for supercapacitors. In addition, the highly flexible fiber membrane is an ideal template for the facile construction and fabrication of various hollow-structured conducting polymers, which may be promising for high-performance electrochemical devices.

2. EXPERIMENTAL SECTION

Materials. Pyromellitic dianhydride (PMDA), 4,4′-oxidianiline (ODA), and *N*,*N*-dimethylacetamide (DMAc) were commercially obtained from China Medicine Co. Aniline and ammonium persulfate (APS) were purchased from Sinopharm Chemical Reagent Co. Ltd. All other reactants were of analytical purity and used as received.

Preparation of Electrospun PAA Nanofiber Membranes. The precursor of polyimide, PAA, was synthesized via the polycondensation of PMDA and ODA with an equivalent molar ratio in DMAc at −3 °C, thus obtaining the pristine PAA solution with the solid content of 15%. Electrospinning was carried out using a syringe with a spinneret having a diameter of 0.5 mm at an applied voltage of 18−25 kV. The PAA solution was fed at a speed of 0.25 mL h^{-1} with a distance of 20 cm between the tip of the needle and the collector.[29]

Preparation of Hollow PANI Nanofibers. The in situ polymerization of aniline was carried out in an ice/water bath at the temperature of 0−5 °C. The as-prepared electrospun PAA fiber membrane was first immersed in 20 mL of 1 M HCl solution containing aniline for the sufficient adsorption of aniline by PAA nanofibers. Then, another 20 mL of 1 M HCl solution containing APS was slowly added into the above solution to initiate the polymerization. Different aniline concentrations of 0.01, 0.03, and 0.05 M were used for polymerization over 12 h, respectively, with the molar ratio of aniline/APS fixed at 2/1. The as-prepared PAA/PANI core/shell nanofibers were thoroughly washed with DMAc to remove the PAA core. Thus, hollow PANI nanofibers with different diameters were obtained and correspondingly marked as H-PANI 1#, 2#, and 3# for the above three aniline concentrations. Meanwhile, for a comparative study, PANI powder was in situ polymerized under the same condition but without the template and marked as P-PANI. The preparation procedure of hollow PANI nanofibers was schematically shown in Figure 1.

Characterization. The morphology of PAA, PAA/PANI, and hollow PANI nanofibers was investigated by a scanning electron microscope (SEM, Tescan) at an acceleration voltage of 20 kV. X-ray diffraction (XRD) experiments were conducted on an X'Pert Pro X-ray diffractometer with Cu Kα radiation (λ = 0.1542 nm) under a voltage of 40 kV and a current of 40 mA. Fourier transform infrared (FTIR) spectra were obtained in the range of 4000−400 cm^{-1} with a 4 cm^{-1} spectral resolution on a Nicolet Nexus 470 spectrometer equipped with a DTGS detector by signal-averaging 64 scans using the KBr pellet technique.

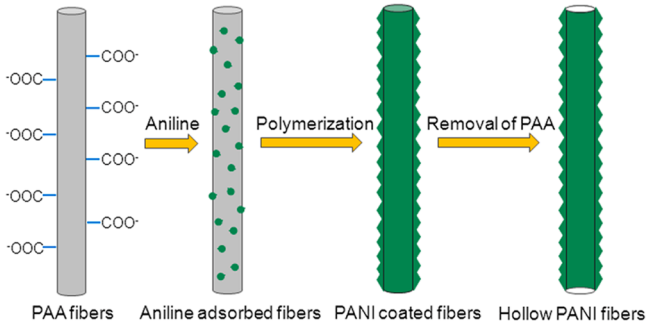

Figure 1. Schematic of the preparation procedure of hollow PANI nanofibers.

All electrochemical experiments were carried out on a CHI 660D electrochemical workstation at room temperature. In the three-electrode system, the samples were used as the working electrode, platinum foil as the counter electrode, Ag/AgCl electrode as reference electrode, and 1.0 M H_2SO_4 aqueous solution as electrolyte. Cyclic voltammetry (CV) curves were obtained in the potential range of −0.2 to 0.8 V vs Ag/AgCl by varying the scan rate from 10 to 100 mV s^{-1}. Galvanostatic charge−discharge measurements were carried out by chronopotentiometry (CP) at 1 to 10.0 A g^{-1}. The capacitance was calculated from the discharge curves, according to the equation $C_s = I^*\Delta t/(m^*\Delta V)$,[30] where C_s is the specific capacitance, I is the constant discharge current, Δt is the discharge time, m is the mass of PANI in a single electrode, and ΔV is the discharge voltage.

3. RESULTS AND DISCUSSION

Structure and Morphology of Hollow PANI Nanofibers. The morphologies of hollow PANI nanofibers were investigated by SEM. As shown in Figure 2a, the diameter of the as-prepared PAA nanofibers is uniform with an average size of about 300 nm. After in situ polymerization of aniline, a thin layer of PANI is grown onto the surface of PAA fibers to form a

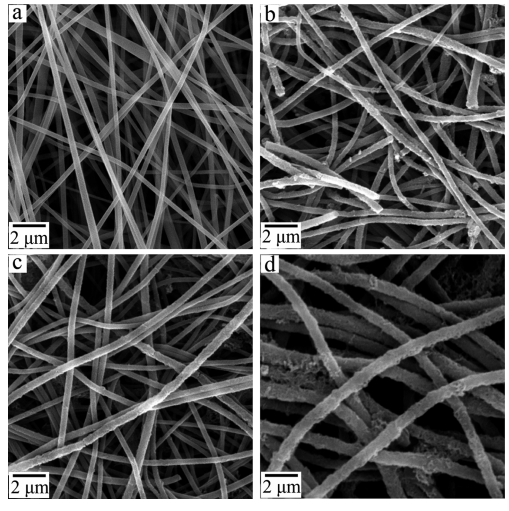

Figure 2. SEM images of (a) PAA fibers, (b) PAA/PANI 1#, (c) PAA/PANI 2#, and (d) PAA/PANI 3# core/shell fibers.

dx.doi.org/10.1021/am4008352 | ACS Appl. Mater. Interfaces 2013, 5, 4423−4428

coaxial structure. The ability to capture aniline monomers in aqueous solutions through electrostatic attraction by PAA is beneficial for the formation of a thin and uniform layer of PANI on the surface of electrospun PAA fibers. From Figure 2b–d, it can be seen that the diameters of PAA/PANI 1#, 2#, and 3# core/shell fibers are about 400, 450, and 550 nm, respectively. When PAA fibers were removed as the sacrificial template, hollow PANI nanofibers were obtained as shown in Figure 3.

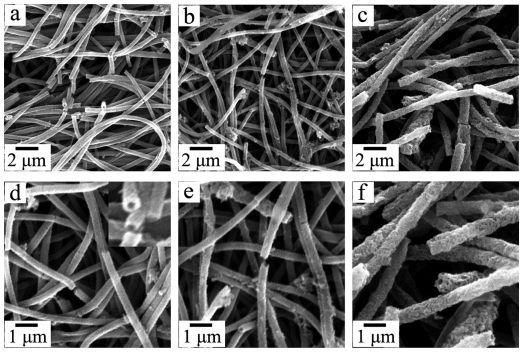

Figure 3. Low and high magnification SEM images of (a, b) H-PANI 1#; (c, d) H-PANI 2#; (e, f) H-PANI 3#.

An enlarged image of the hollow-structured fibers is also provided in the inset of Figure 3d. From the diameter change of the fibers before and after in situ polymerization of aniline, the wall thicknesses of H-PANI 1#, 2#, and 3# samples are calculated to be 50, 75, and 125 nm, respectively. However, large PANI agglomerates are gradually formed when the initial concentration of aniline is over 0.03 M, which may be attributed to the rapid nucleation and polymerization of aniline in the solution. Thus, it can be concluded that the wall thickness of hollow PANI nanofibers can be well controlled by adjusting the initial concentration of aniline. Moreover, the high flexibility of the self-standing fiber membrane makes it an ideal template for the facile construction and fabrication of PANI and other conducting polymers with hollow structures.

XRD was employed to monitor the structure of P-PANI and H-PANI 1# samples. As shown in Figure 4, the diffraction peaks at 2θ = 9.8° and 15.3° are the characteristic repeating units and doping diffraction peaks of PANI, while the peaks centered at 2θ = 20.9° and 25.9° are ascribed to the periodicity parallel and perpendicular to PANI chains, respectively.[31,32]

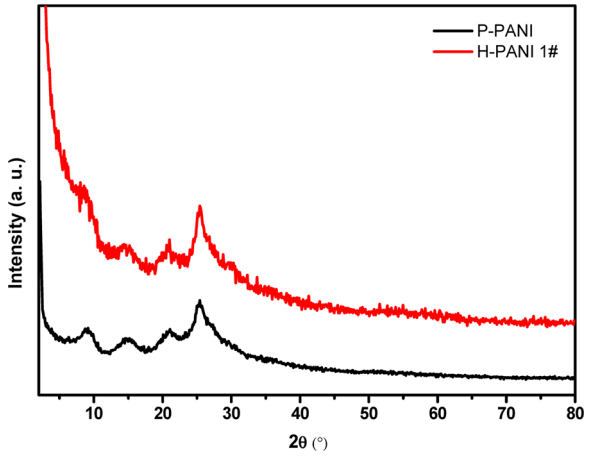

Figure 4. XRD patterns of P-PANI and H-PANI 1#.

These results demonstrate a successful in situ polymerization of aniline in the presence of PAA nanofiber template. FTIR spectrum of H-PANI 1# further confirms the formation of PANI (Figure 5). The absorption band at 3443 cm^{-1}

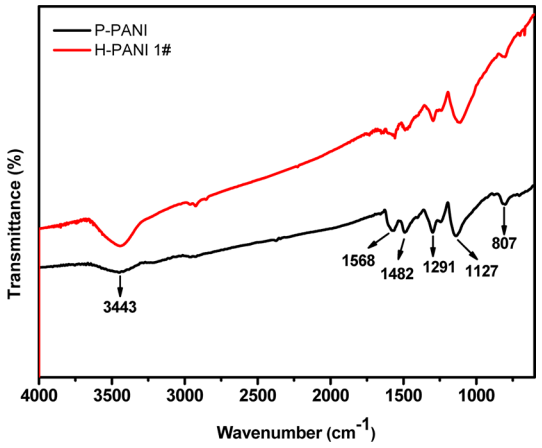

Figure 5. FTIR spectra of P-PANI and H-PANI 1#.

corresponds to the N–H stretching of aromatic amines. The characteristic peaks at 1568 and 1482 cm^{-1} are attributed to the C–C stretching of the quinonoid (Q) and benzenoid (N) rings of PANI, respectively. The bands at 1291 and 1242 cm^{-1} are assigned to the C–N stretching of the benzenoid ring while the N–Q–N stretching at 1127 cm^{-1} is the characteristic band of polyaniline salt.

Electrochemical Properties of Hollow PANI Nanofibers. CV measurements were performed to study the capacitive performance of PANI powder and hollow nanofiber electrodes. As shown in Figure 6, the CV curves of both PANI

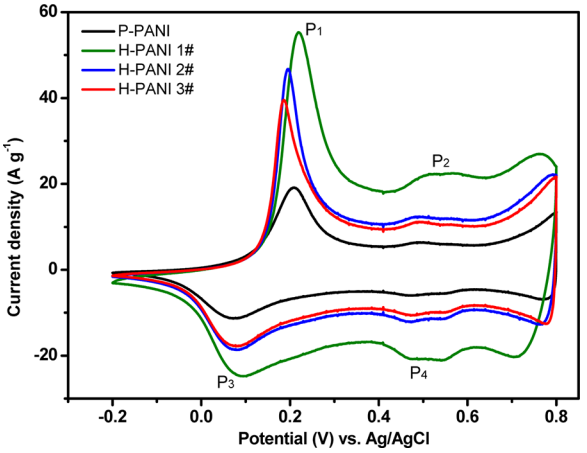

Figure 6. CV curves of P-PANI, H-PANI 1#, H-PANI 2#, and H-PANI 3# in 1 M H_2SO_4 at scan rate of 20 mV s^{-1} from −0.2 to 0.8 V (vs Ag/AgCl).

powder and hollow nanofiber electrodes display two pairs of redox peaks (P_1/P_3, P_2/P_4), which imply the reversible charge–discharge behavior and pseudocapacitance characteristics. The ideal capacitor-like behavior can be attributed to the redox transformations of PANI: the leucoemeraldine–emeraldine (P_1/P_3) and emeraldine–pernigraniline (P_2/P_4) transformations. From Figure 6, it can be seen that the peak currents of all hollow PANI nanofibers are higher than that of PANI powder,

dx.doi.org/10.1021/am4008352 | ACS Appl. Mater. Interfaces 2013, 5, 4423–4428

indicating an obviously improved capacitance. In addition, the peak current densities of the three hollow PANI nanofiber electrodes gradually increased, with H-PANI 1# showing the highest peak current density. As aforementioned, the wall thickness of hollow PANI nanofibers increases with the increase of initial concentration of aniline. H-PANI 1# obtained under lower initial concentration of aniline exhibits smaller wall thickness of 50 nm, which can result in higher surface area and better utilization of PANI. For H-PANI 2# and 3#, large agglomerates of PANI are gradually covering the nanofiber surface, which can reduce the accessible surface area and hinder the ion diffusion process. Therefore, H-PANI 1# exhibits the highest peak current density during the CV measurements. Furthermore, CV curves of H-PANI 1# at different scan rates were performed in the given potential range. With the scan rate increasing from 10 to 100 mV s^{-1} (Figure 7), the cathodic

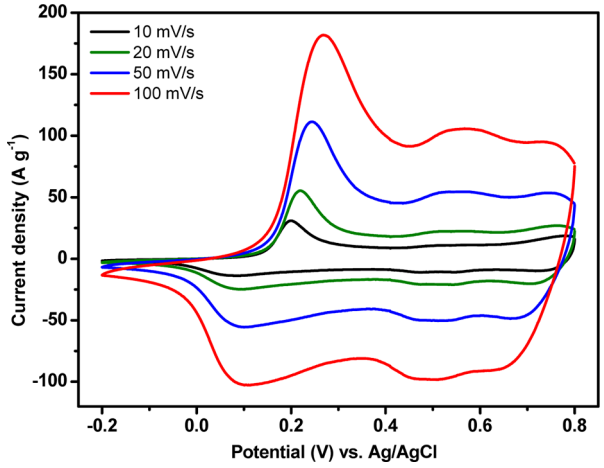

Figure 7. CV curves of H-PANI 1# at different scan rates in 1 M H_2SO_4 from −0.2 to 0.8 V (vs Ag/AgCl).

peaks (P_1, P_2) shift positively and the anodic peaks (P_3, P_4) shift negatively, respectively, indicating good rate ability and ideal capacitance behavior for the hollow PANI nanofiber electrodes.

The charge−discharge performance is investigated by CP in the potential range of 0−0.8 V. As shown in Figure 8, the symmetry of all the charge and discharge curves reveals good

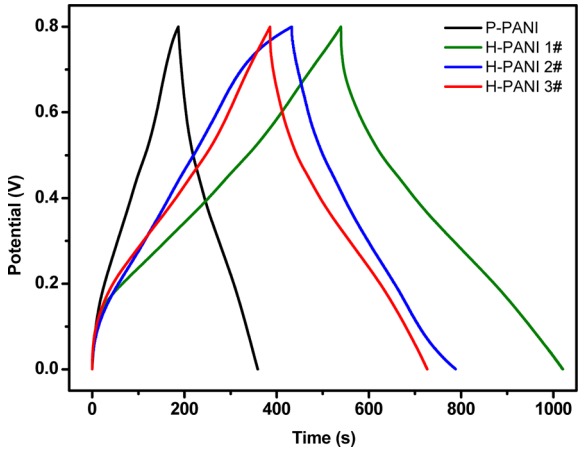

Figure 8. Charge/discharge curves of P-PANI, H-PANI 1#, H-PANI 2#, and H-PANI 3# at a current density of 1 A g^{-1}, respectively.

capacitance characteristics. According to the capacitance equation evaluated from the discharge curves, the specific capacitances of PANI powder and H-PANI 1#, 2#, and 3# hollow nanofibers at 1 A g^{-1} are calculated to be 216, 601, 450, and 426 F g^{-1}, respectively. The capacitance of hollow PANI nanofibers is significantly improved compared with that of PANI powder. In addition, the capacitance of hollow PANI nanofibers increases with the decrease of the initial concentration of aniline. As the pseudocapacitance of PANI is derived from the redox reaction involving the influx and outflux of electroactive ions from the polymer, the ion diffusion in PANI electrode plays a vital role in determining the performance of supercapacitors.[33,34] Typically, the in situ polymerized PANI powder in aqueous solution is prone to form densely packed geometry with less accessible surface area, thus limiting the penetration of electroactive ions far inside the PANI and resulting in lower utilization of the conducting polymer in the charge storage process. When PANI is loaded onto the surface of PAA nanofibers, the distribution of densely packed PANI can be obviously improved, forming hollow nanostructures. These ordered hollow passages provide numerous channels and large contact area, which facilitates the effective penetration of the electrolyte and ensures high utilization of the conducting polymer. Moreover, H-PANI 1# with thinner wall thickness exhibits higher capacitance of 601 F g^{-1} at 1 A g^{-1}, which can be attributed to the shortened charge transport distance of the electroactive ions into the far inner layer of PANI. The specific capacitance of H-PANI 1# (601 F g^{-1} at 1 A g^{-1}) is much higher than those previously reported, such as PANI coated hollow carbon sphere composites (525 F g^{-1} at 0.1 A g^{-1})[16] and PANI/graphene oxide multilayer films (375.2 F g^{-1} at 0.5 A g^{-1}),[35] making it promising for high-performance supercapacitors.

The rate capability is investigated under different charge−discharge current densities as shown in Figure 9. With

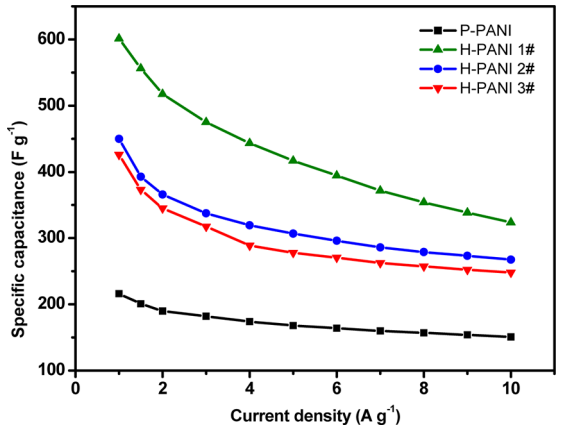

Figure 9. Specific capacitance plots of P-PANI, H-PANI 1#, H-PANI 2#, and H-PANI 3# at different current densities, respectively.

increasing current density, the capacitances of both PANI powder and hollow nanofibers decrease. Nevertheless, the capacitances of all PANI hollow nanofibers are still much higher than that of PANI powder at all current densities. As is known, the diffusion rate of the electrolyte is drastically slowed down under high current densities, which result in the ions only penetrating into the inner surface of the relatively large pores and less active surface area of the electrode material taking part in the charge−discharge processes.[13] Compared with the

densely packed PANI powder, the porous and thin tubular structure of hollow PANI nanofibers makes the penetration of the electrolyte ions into the inner surface of the active electrode material easier. Therefore, the capacitances of H-PANI 1#, 2#, and 3# are maintained at 324, 268, and 248 F g^{-1}, respectively, even at a high current density of 10 A g^{-1}.

Furthermore, the electrochemical stability of hollow PANI nanofibers was evaluated by galvanostatic charge−discharge measurements at a current density of 1 A g^{-1}. As shown in Figure 10, H-PANI 1# keeps a higher retention ratio of 62%

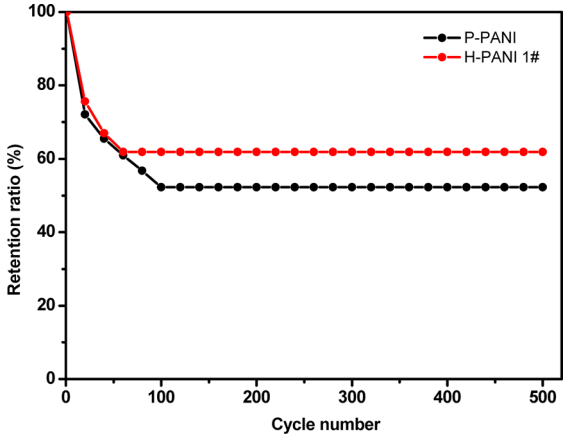

Figure 10. Plots of cycle life test of P-PANI and H-PANI 1# at a current density of 1 A g^{-1}.

(373 F g^{-1}) compared with that (52%, 112 F g^{-1}) of PANI powder after 500 cycles. However, the retention ratio of hollow PANI nanotubes is still far from the ideal value of 100%, which may be attributed to the cracking or breaking of the hollow nanotubes during the charge−discharge process. The hollow polyaniline nanofibers without any protection layers cannot effectively prohibit the contraction/expansion of polyaniline. Therefore, hollow-structured PANI nanofiber composites with improved mechanical and cycling performance will be more promising for high-performance supercapacitors.

4. CONCLUSIONS

In summary, hollow PANI nanofibers with controllable wall thickness have been successfully obtained by in situ polymerization of aniline using the electrospun PAA nanofiers as a template. The hollow structure, thin wall thickness, and orderly pore passages can facilitate the ion diffusion and improve the utilization of the electroactive PANI during the charge−discharge processes, which significantly improve the electrochemical performance of hollow PANI nanofibers. By using the highly flexible fiber membrane as a template, it provides possibilities for the facile construction and fabrication of conducting polymers with hollow structures, which may find potential applications in various high-performance electrochemical devices.

AUTHOR INFORMATION

Corresponding Author

*Tel: 86-21-55664197. Fax: 86-21-65640293. E-mail: txliu@fudan.edu.cn.

Notes

The authors declare no competing financial interest.

ACKNOWLEDGMENTS

The authors are grateful for the financial support from the National Natural Science Foundation of China (51125011).

REFERENCES

(1) Miller, J. R.; Simon, P. *Science* **2008**, *321*, 651−652.
(2) Liu, C.; Li, F.; Ma, L.-P.; Cheng, H.-M. *Adv. Mater.* **2010**, *22*, E28−E62.
(3) Zhao, L.; Fan, L.-Z.; Zhou, M.-Q.; Guan, H.; Qiao, S.; Antonietti, M.; Titirici, M.-M. *Adv. Mater.* **2010**, *22*, 5202−5206.
(4) Chen, L.-F.; Zhang, X.-D.; Liang, H.-W.; Kong, M.; Guan, Q.-F.; Chen, P.; Wu, Z.-Y.; Yu, S.-H. *ACS Nano* **2012**, *6*, 7092−7102.
(5) Ghosh, S.; Inganäs, O. *Adv. Mater.* **1999**, *11*, 1214−1218.
(6) Yan, X.; Tai, Z.; Chen, J.; Xue, Q. *Nanoscale* **2011**, *3*, 212−216.
(7) Domingues, S. H.; Salvatierra, R. V.; Oliveira, M. M.; Zarbin, A. J. G. *Chem. Commun.* **2011**, *47*, 2592−2594.
(8) Lai, X. Y.; Halperta, J. E.; Wang, D. *Energy Environ. Sci.* **2012**, *5*, 5604−5618.
(9) Tang, X.; Liu, Z.-H.; Zhang, C.; Yang, Z.; Wang, Z. *J. Power Sources* **2009**, *193*, 939−943.
(10) Chen, H.; Zhou, S. X.; Chen, M.; Wu, L. M. *J. Mater. Chem.* **2012**, *22*, 25207−25216.
(11) He, S.; Hu, X.; Chen, S.; Hu, H.; Hanif, M.; Hou, H. *J. Mater. Chem.* **2012**, *22*, 5114−5120.
(12) Luo, X.; Killard, A. J.; Morrin, A.; Smyth, M. R. *Chem. Commun.* **2007**, 3207−3209.
(13) Wang, J.-G.; Yang, Y.; Huang, Z.-H.; Kang, F. *J. Power Sources* **2012**, *204*, 236−243.
(14) Wang, K.; Huang, J.; Wei, Z. *J. Phys. Chem. C* **2010**, *114*, 8062−8067.
(15) Wang, Z.-L.; Guo, R.; Li, G.-R.; Lu, H.-L.; Liu, Z.-Q.; Xiao, F.-M.; Zhang, M.; Tong, Y.-X. *J. Mater. Chem.* **2012**, *22*, 2401−2404.
(16) Lei, Z.; Chen, Z.; Zhao, X. S. *J. Phys. Chem. C* **2010**, *114*, 19867−19874.
(17) Cao, Y.; Mallouk, T. E. *Chem. Mater.* **2008**, *20*, 5260−5265.
(18) Zhang, M.; Shao, C.; Guo, Z.; Zhang, Z.; Mu, J.; Cao, T.; Liu, Y. *ACS Appl. Mater. Interfaces* **2011**, *3*, 369−377.
(19) Miao, Y.-E.; Wang, R. Y.; Chen, D.; Liu, Z. Y.; Liu, T. X. *ACS Appl. Mater. Interfaces* **2012**, *4*, 5353−5359.
(20) Fang, X.; Xiao, S.; Shen, M.; Guo, R.; Wang, S.; Shi, X. *New J. Chem.* **2011**, *35*, 360−368.
(21) Wang, X.; Wang, J.; Si, Y.; Ding, B.; Yu, J. Y.; Sun, G.; Luo, W.; Zheng, G. *Nanoscale* **2012**, *4*, 7585−7592.
(22) Ren, T.; Si, Y.; Yang, J.; Ding, B.; Yang, X.; Hong, F.; Yu, J. Y. *J. Mater. Chem.* **2012**, *22*, 15919−15927.
(23) Wang, X.; Si, Y.; Wang, X.; Yang, J.; Ding, B.; Chen, L.; Hu, Z.; Yu, J. Y. *Nanoscale* **2013**, *5*, 886−889.
(24) Mu, J.; Chen, B.; Guo, Z.; Zhang, M.; Zhang, Z.; Zhang, P.; Shao, C.; Liu, Y. *Nanoscale* **2011**, *3*, 5034−5040.
(25) Zhi, M.; Manivannan, A.; Meng, F.; Wu, N. *J. Power Sources* **2012**, *208*, 345−353.
(26) Huang, C.; Wang, S.; Zhang, H.; Li, T.; Chen, S.; Lai, C.; Hou, H. *Eur. Polym. J.* **2006**, *42*, 1099−1104.
(27) Carlberg, B.; Ye, L.-L.; Liu, J. *Small* **2011**, *7*, 3057−3066.
(28) Yang, S.; Wu, D.; Qi, S.; Cui, G.; Jin, R.; Wu, Z. *J. Phys. Chem. B* **2009**, *113*, 9694−9701.
(29) Chen, D.; Liu, T. X.; Zhou, X. P.; Tjiu, W. W.; Hou, H. Q. *J. Phys. Chem. B* **2009**, *113*, 9741−9748.
(30) Reddy, A. L. M.; Ramaprabhu, S. *J. Phys. Chem. C* **2007**, *111*, 7727−7734.
(31) Cheng, F. Y.; Tang, W.; Li, C. S.; Chen, J.; Liu, H. K.; Shen, P. W.; Dou, S. X. *Chem.—Eur. J.* **2006**, *12*, 3082−3088.
(32) Zhang, L.; Wan, M. *Adv. Funct. Mater.* **2003**, *13*, 815−820.
(33) Yan, J.; Khoo, E.; Sumboja, A.; Lee, P. S. *ACS Nano* **2010**, *4*, 4247−4255.
(34) Xing, W.; Qiao, S. Z.; Ding, R. G.; Li, F.; Lu, G. Q.; Yan, Z. F.; Cheng, H. M. *Carbon* **2006**, *44*, 216−224.

(35) Lee, T.; Yun, T.; Park, B.; Sharma, B.; Song, H.-K.; Kim, B.-S. *J. Mater. Chem.* **2012**, *22*, 21092−21099.